CHAPTER 3

Computational modeling of the thin muscle layer, panniculus carnosus, demonstrates principles of pressure injury and prophylactic dressings

Bryan Wee Siang Soh[1], **Alberto Corrias**[1], **Lisa Tucker-Kellogg**[2,3]
[1]*Department of Biomedical Engineering, National University of Singapore, Singapore;*
[2]*Centre for Computational Biology, Duke-NUS Medical School, Singapore;*
[3]*Cancer and Stem Cell Biology, Duke-NUS Medical School, Singapore*

Chapter Outline

1. Introduction

Pressure ulcers (PUs, also called pressure injuries) are areas of soft tissue breakdown that result from sustained mechanical loading of the skin and the underlying tissues. The loading may be direct pressure or pressure with shear or friction force [1]. A PU arises when some regions of soft tissue undergoe cell death in response to the sustained pressure [2].

The etiology of PUs requires greater understanding to provide efficient prevention and therapy, and more research is necessary [3]. Possible mechanisms of injury include ischemia (disrupted blood flow), reperfusion, rupture of cellular structures, metabolic stress, and oxidative stress. Ischemic injury can result from direct sustained pressure, from repetitive moderate pressure, and/or from shear. When ischemia is followed by reperfusion

Innovations and Emerging Technologies in Wound Care. https://doi.org/10.1016/B978-0-12-815028-3.00003-1

of blood, the ischemia–reperfusion combination causes oxidative stress and tissue injury [4]. Another important mechanism of tissue injury during PU formation is increased membrane permeability or outright rupture of cell membranes [5,6]. The integrity of cell plasma membranes (the sarcolemma in muscle cells [7]) is required for health and homeostasis, and if a cell membrane experiences a large rupture, the cell undergoes lysis and death. The cellular contents released from cell lysis may include alarmins that trigger inflammation or redox active compounds such as globin proteins, which can create oxidative stress, alone or in combination with other proteins in the wound [8]. The cytoskeleton of a healthy cell has a remarkable capacity for dynamic remodeling and flexible geometry [9]. Cellular stress response signaling can help cells survive harsh conditions [10], often with transient dynamics [11], and the same pathways can make cells vulnerable to prodeath stimuli through the pathways of extrinsic apoptosis [12,13]. Extracellular matrix architecture may provide considerable protection for mechanical stability, but the extracellular matrix is in constant flux, and the mechanical capability of extracellular matrix can be decreased if there is a jump in protease activity [14]. In summary, many biological processes may contribute to injury, and more research must be focused on the PU context rather than speculated by analogy from other contexts.

As improvements in medical care allow people to live longer with comorbid conditions, immobility becomes an increasingly prevalent problem [15]. Care of immobile people requires frequent turning to prevent PU formation in vulnerable areas [16]. Despite the significant costs to stakeholders and the efforts invested in prevention/education, PU occurrence remains a serious problem. An American study reported that there are 2.5 million new cases of PUs every year, with an annual cost of USD 11.6 billion, and 60,000 patient deaths due to PUs annually [17]. Turning and off-loading can be achieved through direct repositioning and/or by use of specialized support surfaces [18], and interest has grown dramatically in the use of prophylactic dressings [19]. Preoperative preparation of surgical patients [20] has been a particularly attractive context for early stage trials of dressings, where the incremental cost is easily accommodated. Lessons learned from early efforts with prophylactic dressings may later extend to a broader variety of PU contexts.

The heels are the most common site for PUs acquired in long-term acute care facilities [21] and are the second most common site for PUs overall (23.6%), after the sacrum (28%) [22]. The heels are also the site where deep tissue injury is most prevalent [16,23,24]. As with other PUs, heel ulcers can involve serious, life-threatening complications [25]. The dorsal surface of the heel is particularly vulnerable to pressure injury. The plantar surface is well adapted to mechanical loading, including high-impact activity, but the posterior heel is not. Over the heel bone (calcaneus) is only a thin layer of skin and soft tissue [16].

The panniculus carnosus (PC) is a thin layer of muscle present in many mammals and in some areas of the human body [3]. The PC is a muscle just below the skin and attached to the skin, which allows movement of the skin independent of the skeleton or deeper muscles. The animal equivalent of the PC functions to dislodge insects or other noxious agents. The PC is considered vestigial in higher primates, where limbs are long enough to reach around the body. In the human body, specific areas have a PC muscle as a discrete structure with clear presence: the platysma of the neck, the subareolar muscle around the nipple, the dartos of the scrotum, the palmaris brevis of the hand, and the corrugator cutis ani [26]. In other areas, the PC layer may be present, absent, or sparsely present in the form of muscle strands that connect to skin but not a continuous sheet. Multiple authors concur that remnants of the PC are still found in many individuals [27]. Note that human anatomy routinely encompasses enormous variability. For example, the plantaris muscle varies in size from person to person, sometimes as large as 13 cm, but is absent in 7%–20% of individuals [28].

The function of the PC is poorly understood and frequently speculated on. The palmaris brevis is a thin PC muscle layer at the base of the hand, and it is believed to protect the nerves and vessels at the ulnar canal (beside the bone) [29]. On this basis, surgeons are advised to preserve it during hand surgery. The electromyographic function and microanatomy at the base of the hand has been more closely studied than equivalent locations on the heel. The heels of cadavers were studied by Cichowitz et al., who performed microdissections and found thin layers of PC muscle at the subcutaneous level in many individuals [3]. To the best of our knowledge, no study has yet performed a comprehensive survey of the geometric extent of the PC in human heels. They proposed that the PC may be the site of origin for PUs of the heel because muscle, as a tissue type, is comparatively vulnerable to ischemic death. From this viewpoint, people with a PC layer in the heel may be more susceptible to pressure injuries. Another viewpoint arose from studying the contractures caused by the PC after burn trauma; Greenwood hypothesized [26] that the PC may have an adaptive function to accelerate wound closure by contracting wound edges. The viewpoint inspired by the palmaris brevis instance (above) suggests the PC may serve as mechanical protection for softer structures near bone. It is this protective capability we wish to consider further in this chapter. Our approach will employ computational biomechanics, simulating finite element models of mechanical deformation and comparing two models: one with the PC and one without.

Prior research in computational biomechanics has generated many insights into the etiology and pathophysiology of heel PUs. In understanding the biomechanics of heel ulcers, mathematical models and finite element simulations have shown stress–strain behaviors of the heel under loading conditions [18,25,30,31]. This has improved understanding of tissue deformation and also the role of support surfaces or external measures to decrease the loading or to improve the load distribution. The simplest

biomechanical model for studying PU risk in heels was constructed using the curved shape of the posterior calcaneus as a rigid sphere that compresses a soft and elastic tissue layer [25]. The abstract geometry of such models is extremely simple approximations of the natural phenomenon. Subsequent work from Luboz et al. performed a 3D simulation and examined internal Von Mises strains resulting from pressures applied to the foot sole to simulate a standing position [30]. The improvements of later work included more detailed models with full bone structure for a foot in addition to tendons and ligaments, including four layers: plantar skin, nonplantar skin, arch muscles, and fat between layers, all with different Neo-Hookean properties [30]. The geometry of these regions was constructed using MRI scans of subjects and can be considered a high-order approximation. This state-of-the-art work is costly to construct. For the question we address here, about the mechanical implications of having a PC layer at the heel, we seek a first-order approximation, more detailed than an abstract sphere and less costly than a clinically customized high-order model.

Another recent contribution aids our work by providing data about heel microanatomy. Cichowitz and Ashton [3] performed careful examination of foot vasculature and, in the course of that effort, came across important evidence about the PC. They found a thin PC muscle layer located within the soft tissue of the heel, just under the dermis of their subjects. Their quantification of PC geometry in the heel is our primary source of PC data. However, because their focus was the whole foot vasculature, they assessed the presence or geometry of a PC layer neither specifically at the posterior aspect of the heel nor in the transition from plantar to posterior surface. Because the dorsal (posterior) surface has very high risk of PU formation, these areas require additional study.

The high prevalence and human cost of PUs creates urgent need for improved methods of risk assessment. If the presence of a PC layer does redistribute biomechanical stress in soft tissues of the heel, as we hypothesize, then clinical imaging of the PC anatomy through means such as ultrasound might one day contribute to improved methods of risk assessment. In the meanwhile, we should not presume to know the net effect of PC anatomy on tissue viability. The firm elasticity of PC tissue might provide some protection of soft structures near bone, when loading is low enough to avoid ischemia of the muscle. On the other hand, the vulnerability of muscle tissue to ischemic injury, and the cytotoxic effects of muscle death on surrounding tissues, might cause harm during the prolonged static stress of immobility [3]. Mechanistically grounded principles for risk assessment will be important to develop, but we also need more tools for prevention, in cases where high risk has been identified. Prophylactic dressings are gaining momentum for prophylaxis of pressure injury [19], and interest may continue to grow if evidence of efficacy accumulates. The biomechanical engineering of dressings to prevent pressure injury is a relatively new field of research, and the field might benefit from biomimetic designs. If the PC has naturally evolved to play some protective function, or if our

simulations show it improves load distribution, then PC anatomy may offer inspiration for the design of prophylactic dressings. This is particularly attractive option because a PC-like dressing on the outer surface of the skin might provide biomechanical protection similar to a natural PC layer under the skin, but unlike natural muscle, the dressing would not become ischemic, necrotic, or toxic after high stress.

2. Methods

2.1 Three-dimensional model of the heel

The three-dimensional (3D) geometry of our model with discrete surface layers (Fig. 3.1) was constructed in Solidworks (CAD software suite) using published values for the physical dimensions of different layers [3,27,32]. Our heel model uses simple geometrical volumes to provide a first-order approximation of the bone, tendon, soft tissue, and skin. A cylinder is used to model the lower leg, and a sphere is used to model the heel bone (calcaneus). To model the slight elevation of the lower leg from the plane, the sphere is rotated 100° instead of 90° from the coronal plane. Figs. 3.1 and 3.2 below show the 3D model of the heel constructed and used in the simulation.

The pressure applied to the calcaneus is intended to mimic the weight of one foot (2 kg), so the force was simulated to be 20 N (Fig. 3.3).

To simulate attachments between each tissue layer, the layers were merged into one solid with different mechanical properties in each region. To simulate pressure originating specifically from the calcaneus bone, we constructed the calcaneus as a separate object. The connections between bone and surrounding tissues are difficult to model because they

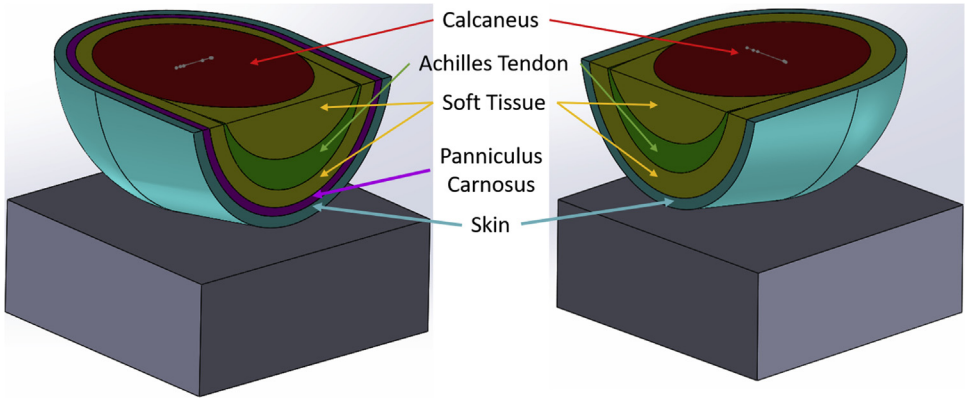

Figure 3.1: Three-dimensional geometry of the heel model, with panniculus carnosus (PC) muscle layer (left) or without (right).

The model without PC has a thicker layer of soft tissue layer, in place of the PC layer. For this and future images, red denotes bone, yellow denotes adipose-like soft tissue, green denotes tendon, purple denotes PC, and turquoise denotes skin.

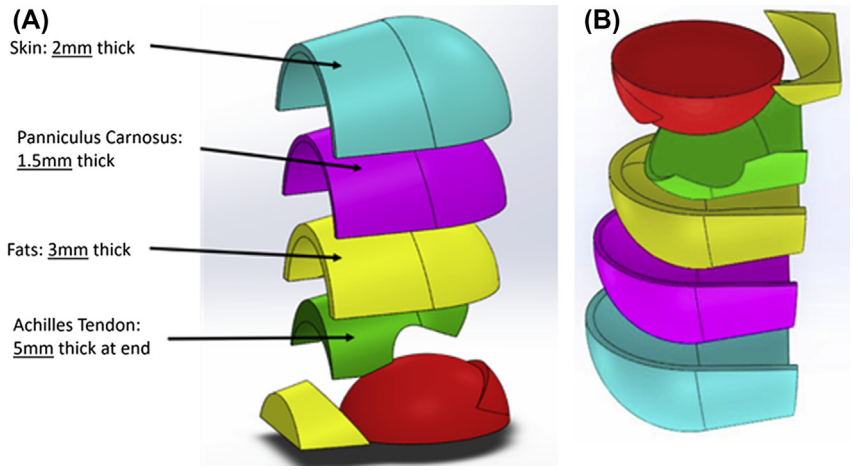

Figure 3.2: Geometry of the model layers.
(A) The thickness of each layer is annotated on an inverted orientation (skin on top and the calcaneus at the bottom) viewed from the medial–lateral perspective. (B) The same model is shown in upright orientation.

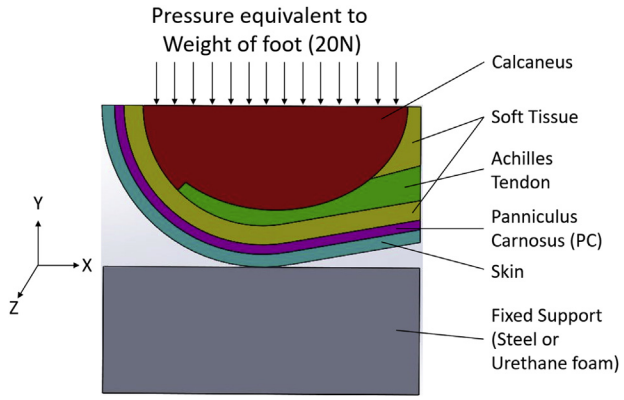

Figure 3.3: Load applied to the bone.
Schematic of simulated force, with constant pressure placed on the calcaneus and transmitted through the heel layers to a base surface. This configuration is intended to induce sustained deformation of the tissues, similar to that of a patient lying supine.

arise through many discrete microscale attachments to filamentous structures. As a macroscale approximation of the adhesion between bone and surrounding tissues, we introduced artificial friction (coefficient 1.5) that was sufficient to maintain contact along the interface between the bone and the surrounding tissues. Boundary conditions were set to prevent the model from rotating in any axis or displacing out of the frame. The top surface of the model will only displace in the Y direction, and the model will be allowed to expand in the X and Z directions to simulate later expansion of the soft tissue as it is flattened. In the superior surface of the heel, boundary conditions permitted movement

only in the Y direction. This simulates resistance from the tissues present in the superior area of the heel. The bottom surface of the base will have zero rotation and displacement, to hold the model in place.

2.2 Simulations

The 3D assembly created using Solidworks was then imported into Abaqus, a software suite for finite element analysis. Mechanical properties were assigned to each layer as shown in Table 3.1. The model was meshed using tetrahedral rather than hexagonal elements due to sharp angles in the soft tissue layer. We added a base layer with mechanical properties of steel (e.g., the footrest of a standard wheelchair) or urethane foam (e.g., a mattress) [33]. The hard base is expected to accentuate the differences in stress behavior between the two models, and the soft foam is expected to minimize the differences.

Following prior work [31,38,39], we used Neo-Hookean hyperelastic properties (Table 3.2) for the more elastically deformable layers, namely the soft tissue, skin, and muscle. Including this deformability improves the model because strong deformations of the softer layers would violate a general elastic model. Here, the shear modulus of the PC is taken as that of a slack muscle and its bulk modulus (K) is calculated using the shear modulus (G) and poisson ratio (v) according to the following equation:

$$K = \frac{2G(1+v)}{3(1-2v)}$$

Table 3.1: Mechanical properties of tissue layers.

Tissue Layer	Young's Modulus, E (MPa)	Poisson's Ratio, v
Soft tissue [34]	2	0.45
Achilles tendon [35]	520.4	0.49
Bone [36]	20,000	0.42
Base (steel) [37]	210,000	0.3
Urethane [33]	0.025	0.0

Table 3.2: Hyperelastic Neo-Hookean properties of tissue layers.

Tissue Layer	Shear Modulus, G (Mpa)	C10: Shear/2 (Mpa)	Bulk Modulus, K (Mpa)	D1: 2/Bulk (1/Mpa)
Soft tissue (fats) [31]	0.000286	0.000143	0.0285	70.175
Panniculus carnosus	0.0071 [38]	0.00355	0.08019 [39]	24.94
Skin [31]	0.039	0.01695	3.179	0.629

After running simulations with a steel base to simulate a sturdy support, we also ran simulations using the properties of urethane foam, a material commonly used in seating and mattresses. When using Neo-Hookean hyperelastic properties, the simulations took 14–24 h to complete on a PC with Intel I7 4 GHz processor and 16 Gb of RAM.

3. Results

After obtaining the final results of the simulation for the model with PC, we then ran the simulation except using the model without PC. Each pair of simulations was done using the same material properties, with the same boundary conditions and interactions in place, and the only difference was the presence or absence of the PC. In each mesh, there were approximately 18,300 elements generated with 47,000 nodes. A comparison of the stress fields from the simulations can be seen in the heat maps of Figs. 3.4 and 3.5. These heat maps use the same ranges of stress, between 0.00,002 Mpa (blue) to 3 Mpa (red). White/gray denotes any stress greater than 3 Mpa.

Figs. 3.4 and 3.5 show a distinctive difference in stress behavior, depending on the presence/absence of the PC. We focus attention only on the regions were PU can occur (not inside the bone and not outside the body). Specifically, we focus on regions with >3 Mpa of stress in soft tissues layers of the fat, skin, and muscle. The model without the PC experiences this extreme level of stress in a broad column between bone and base, passing through all the tissue layers. In contrast, the model with PC has low stress in skin and only a small region of high stress >3 Mpa in the fatty soft tissue.

After obtaining results for a heel resting on a steel base, we next ran simulations using urethane foam as the base. Models with and without PC were simulated using these

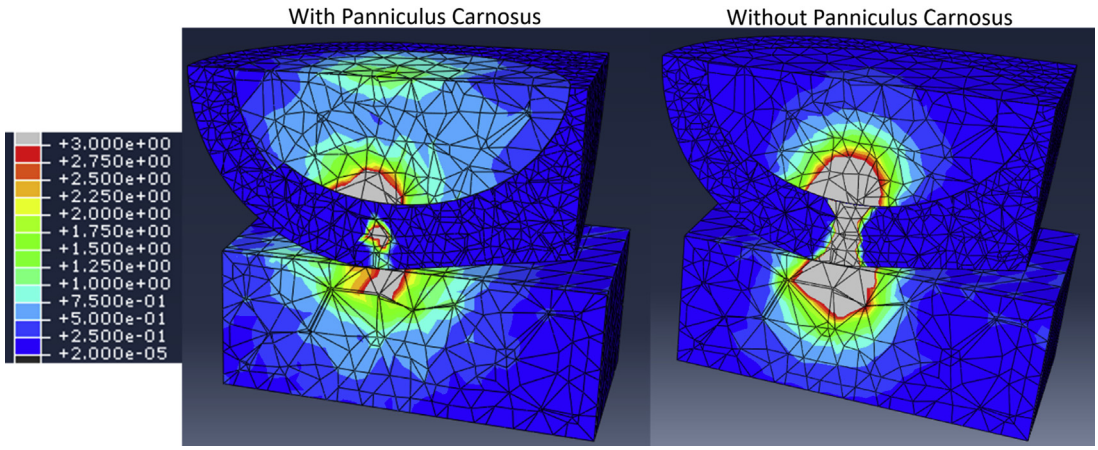

Figure 3.4
Stress heat map of the simulation with steel base. Model is viewed in the X-plane (range is in Mpa).

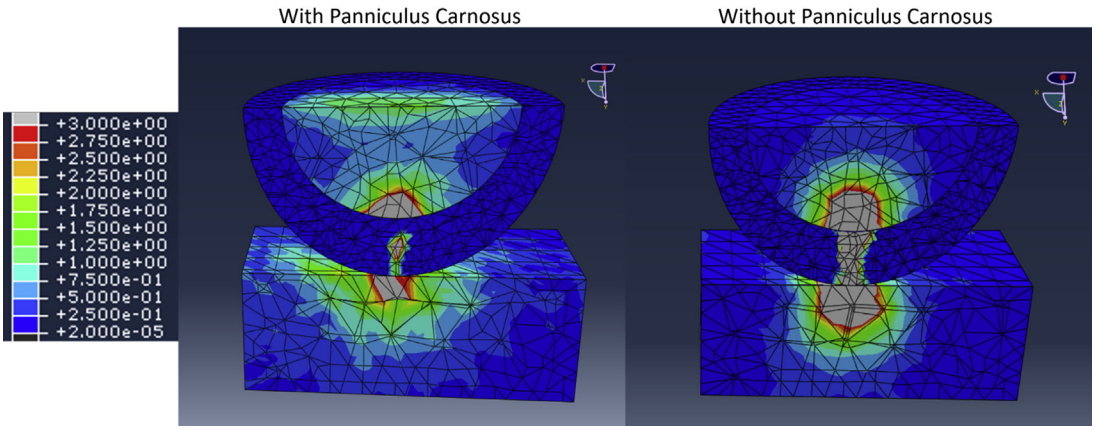

Figure 3.5
Stress heat map of the simulation with steel base. Model is viewed in the Z-plane (range is in Mpa).

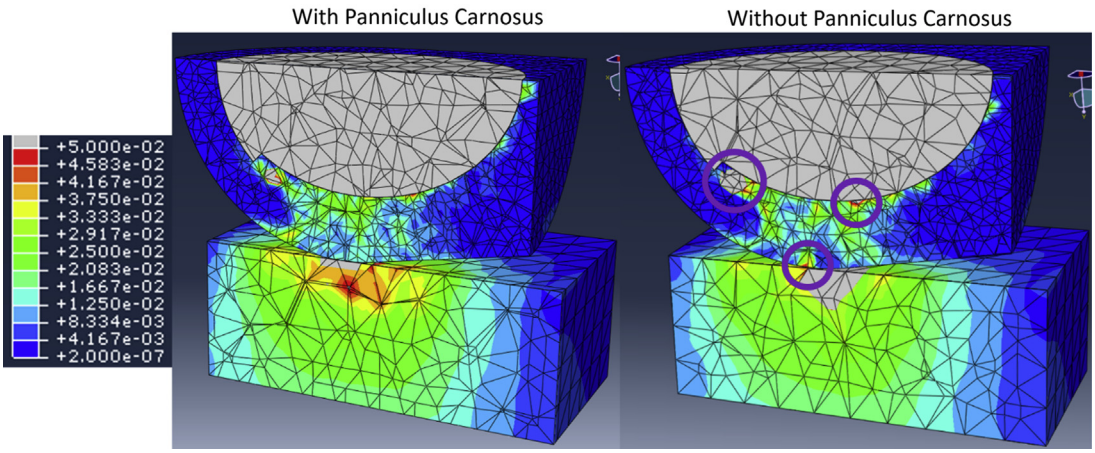

Figure 3.6: Stress heat map of the simulation with urethane foam base.
Model is viewed in the X-plane (range is in Mpa).

conditions (i.e., the same boundary conditions and interactions in place), and all material properties unchanged except the soft base. We calculated the effects of applying 20 N force to the heel bone (mimicking the weight of a foot), and the resulting stress fields are shown as heat maps in Figs. 3.6 and 3.7 below. Compared with the results using a steel base, the heat maps for stress on a foam base show a much lower range of stress values, between 0.0000002 Mpa (blue) and 0.05 Mpa (red). White denotes any stress value above 0.05 Mpa. The calcaneus is colored white because it experiences stress above the mapped range, but this heat map is calibrated for a much lower range than Figs. 3.4 and 3.5.

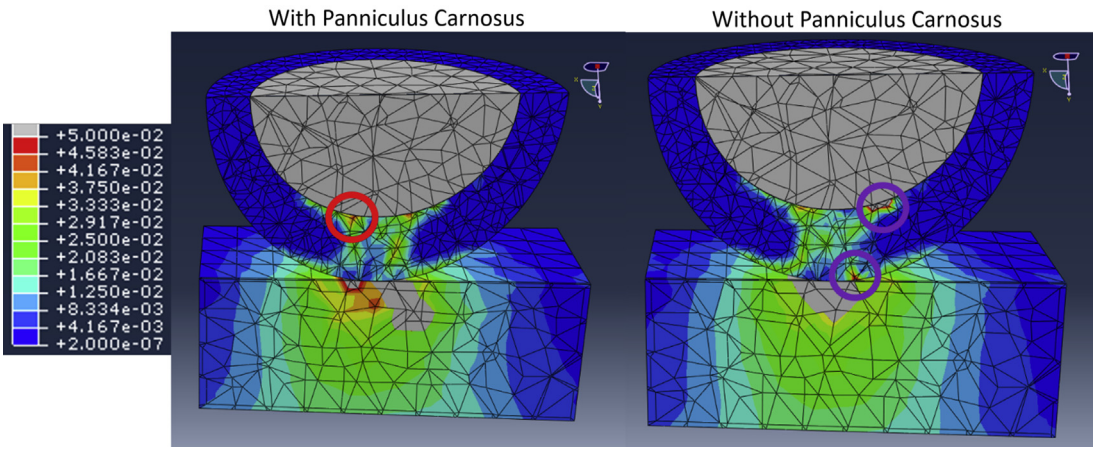

Figure 3.7: Stress heat map of the simulation with urethane foam base.
Model is viewed in the Z-plane (range is in Mpa).

Because the foam surface creates far less stress than steel, the impact of the PC is more subtle. Fig. 3.7 is annotated with circles showing some differences. However, because of meshing and numerical approximation at each node, it is not possible to infer significance from small differences in isolated nodes. Overall, the model without PC still experiences a higher amount of stress in the layers of soft tissue, but this might not have any practical importance when the base support is soft.

4. Discussion

A simplified 3D biomechanical model of heel tissues was developed for determining whether the presence of a firm elastic layer, resembling the PC muscle, would mitigate stresses typical of PU formation. The heel model consists of three large components: a rigid bone, a merged set of nonbone layers (fats, tendon, muscle, and skin; in the model without, the PC will have fats replaced by the muscle layer), and a rigid support surface below. Stress behavior was computed using a biomechanical simulation of the heel on a flat base using the Abaqus software suite.

The results from the biomechanical simulations suggest that there are differences between the two models, when loaded on a hard surface. In the presence of the PC tissue, the heel will experience higher stress in the inner layers of the heel, as seen in the white and red parts in the heat map. In the absence of the PC tissue, we can observe that the heel experiences high stress in a much larger area in surrounding tissues, which spans from the contact at the calcaneus to the contact point at the inferior part of the model. This suggests that the presence of a thin muscle layer can improve the distribution of load during high-stress conditions and motivate us to propose development of PC-like biomimetic

dressings for adhesion to the skin surface. When we run the simulation using a soft base of support, the differences become much smaller, suggesting that the PC is less important to the biomechanics in a well-cushioned context. As expected, dressings to prevent pressure injury would be less likely to bring any benefit in low-stress contexts.

There are several limitations to our approach that need to be considered when deciding whether to pursue development of PC-like dressings for PU prevention. The first is that our model is a first-order approximation of the heel geometry and is not faithful to the anatomical details of a real human heel. The approximation was constructed using published dimensions, but without use of clinical imaging. For example, the fat layer has been modeled to entirely fill a volume that should also contain vasculature and nerves. Although these nonfat components make up a very small faction of the soft tissue volume, they have disproportionate importance, which the current model neglects. Secondly, the mechanical properties of the different tissue types were taken from prior publications with macroscopic mechanics represented by bulk parameters. Such simplifications fail to reflect the complexity of microarchitecture and heterogeneous reality. Although we may aspire to comprehensive parameterization of computational models through empirical fitting of extensive measurements (as for biochemical systems [40]), biomechanical models are only starting to approach authenticity to human patients [41]. A third limitation is the set of interactions between the different layers. Our simulations used high friction to create connection between the calcaneus and the surrounding tissue layers, but future work should improve this approximation. Lastly, the simulated location of the PC is just below the skin, due to the PC being a dermal muscle layer. However, the detailed placement of PC in human heels requires further clarification, especially for its continuation from the plantar to the dorsal side of the heel. Simulations can still be done with different positions of the PC with the current conditions and finite element simulation methods, simply by changing the position of the PC in the 3D model (e.g., using Solidworks software). Future simulations, in conjunction with dressing design and development, should demonstrate the effects of PC-like layers on the external surface of the heel.

In conclusion, we used 3D finite element modeling to run simulations of pressure on a heel-like geometry, and we compared the levels of tissue deformation with and without the PC layer. The presence of the PC caused consistent and extensive decrease in stress experienced by soft tissues resting on a firm surface. This could be due to its elasticity and compressibility, allowing redistribution of the applied forces over larger regions. Future work can provide more detailed models with greater anatomical accuracy, based on dissection or clinical imaging of actual heels, and based on engineered PC-like dressings for adhesion to the epidermis, at the dorsal heel and other vulnerable regions. Understanding our native biology for preventing pressure injury will aid in design of safe and effective interventions such as prophylactic dressings.

Acknowledgments

We are grateful to Sandeep Jacob Sebastin, Ang Eng Tat, Julia H. Jenkins, Elson Neo, and Goh Jia Ling for fruitful discussions about the panniculus carnosus.

We gratefully acknowledge support to LTK from the Singapore Ministry of Health's National Medical Research Council (NMRC) under its Open Fund Individual Research Grant scheme (OFIRG15nov062) and also from the National Research Foundation (NRF), Prime Minister's Office, Singapore, under its CREATE program, Singapore-MIT Alliance for Research and Technology (SMART) BioSystems and Micromechanics (BioSyM) IRG.

References

[1] National Pressure Ulcer Advisory Panel. Pressure definition and stages revised by NPUAP. February 2007. Available at: www.npuap.org/documents/PU_Definition_Stages.pdf.
[2] Barton AA. The pathogenesis of skin wounds due to pressure. J Tissue Viability 2006;16(3):12−5.
[3] Cichowitz A, Pan WR, Ashton M. The heel: anatomy, blood supply, and the pathophysiology of PUs. Ann Plast Surg 2009;62(4):423−9. https://doi.org/10.1097/SAP.0b013e3181851b55.
[4] Kalogeris T, Baines CP, Krenz M, Korthuis RJ. Cell biology of ischemia/reperfusion injury. Int Rev Cell Mol Biol 2012;298:229−317. https://doi.org/10.1016/B978-0-12-394309-5.00006-7.
[5] Jagannathan NS, Tucker-Kellogg L. Membrane permeability during pressure ulcer formation: a computational model of dynamic competition between cytoskeletal damage and repair. J Biomech 2016;49(8):1311−20. https://doi.org/10.1016/j.jbiomech.2015.12.022.
[6] Slomka N, Gefen A. Relationship between strain levels and permeability of the plasma membrane in statically stretched myoblasts. Ann Biomed Eng 2012;40(3):606−18. https://doi.org/10.1007/s10439-011-0423-1.
[7] Nguyen BP, Heemskerk H, So PTC, Tucker-Kellogg L. Superpixel-based segmentation of muscle fibers in multi-channel microscopy. BMC Syst Biol 2016;10(Suppl. 5):124. https://doi.org/10.1186/s12918-016-0372-2.
[8] Bahl N, Winarsih I, Tucker-Kellogg L, Ding JL. Extracellular haemoglobin upregulates and binds to tissue factor on macrophages: implications for coagulation and oxidative stress. Thromb Haemostasis 2014;111(1):67−78. https://doi.org/10.1160/TH13-03-0220.
[9] Venkatraman L, Tucker-Kellogg L. The CD47-binding peptide of thrombospondin-1 induces defenestration of liver sinusoidal endothelial cells. Liver Int 2013;33(9):1386−97. https://doi.org/10.1111/liv.12231.
[10] Umoh NA, Walker RK, Millis RM, Al-Rubaiee M, Gangula PR, Haddad GE. Calcitonin gene-related peptide regulates cardiomyocyte survival through regulation of oxidative stress by PI3K/Akt and MAPK signaling pathways. Ann Clin Exp Hypertens 2014;2(1):1007.
[11] Nim TH, Luo L, White JK, Clément M-V, Tucker-Kellogg L. Non-canonical activation of Akt in serum-stimulated fibroblasts, revealed by comparative modeling of pathway dynamics. PLoS Comput Biol 2015;11(11):e1004505. https://doi.org/10.1371/journal.pcbi.1004505.
[12] Shi Y, Mellier G, Huang S, White J, Pervaiz S, Tucker-Kellogg L. Computational modelling of LY303511 and TRAIL-induced apoptosis suggests dynamic regulation of cFLIP. Bioinformatics (Oxford, England) 2013;29(3):347−54. https://doi.org/10.1093/bioinformatics/bts702.
[13] Tucker-Kellogg L, Shi Y, White JK, Pervaiz S. Reactive oxygen species (ROS) and sensitization to TRAIL-induced apoptosis, in Bayesian network modelling of HeLa cell response to LY303511. Biochem Pharmacol 2012;84(10):1307−17. https://doi.org/10.1016/j.bcp.2012.08.028.
[14] Venkatraman L, Chia S-M, Narmada BC, White JK, Bhowmick SS, Forbes Dewey C, So PT, Tucker-Kellogg L, Yu H. Plasmin triggers a switch-like decrease in thrombospondin-dependent activation of TGF-β1. Biophys J 2012;103(5):1060−8. https://doi.org/10.1016/j.bpj.2012.06.050.

[15] Cheah J. Chronic disease management: a Singapore perspective. BMJ 2001;323(7319):990–3.
[16] Fowler E, Scott-Williams S, McGuire JB. Practice recommendations for preventing heel PUs. Ostomy/Wound Manag 2008;54(10):42–57.
[17] Content last reviewed Are we ready for change. Rockville, MD: Agency for Healthcare Research and Quality; October 2014. https://www.ahrq.gov/professionals/systems/hospital/pressureulcertoolkit/putool1.html.
[18] Levy A, Kopplin K, Gefen A. An air-cell-based cushion for pressure ulcer protection remarkably reduces tissue stresses in the seated buttocks with respect to foams: finite element studies. J Tissue Viability 2014;23(1):13–23. https://doi.org/10.1016/j.jtv.2013.12.005.
[19] Byrne J, Nichols P, Sroczynski M, Stelmaski L, Stetzer M, Line C, Carlin K. Prophylactic sacral dressing for pressure ulcer prevention in high-risk patients. Am J Crit Care 2016;25(3):228–34. https://doi.org/10.4037/ajcc2016979.
[20] Walker R, Aitken LM, Huxley L, Juttner M. Prophylactic dressing to minimize sacral pressure injuries in high-risk hospitalized patients: a pilot study. J Adv Nurs 2015;71(3):688–96. https://doi.org/10.1111/jan.12543.
[21] Van Gilder C, Washienko C, Eckstein A, Decker S, MacFarlane G. International pressure ulcer prevalence survey results for long-term acute care facilities in the United States. 2005. Available at: www.sawc.net/ses/sawc/abstracts/06323.
[22] Van Gilder C, Macfarlane GD, Meyer S. Results of nine international pressure ulcer prevalence surveys: 1989 to 2005. Ostomy/Wound Manage 2008;54(2):40–54.
[23] Black J. Preventing PUs occurring on the heel. Wounds Int 2012;3(3):1–4.
[24] Salcido R. Editorial: what is the purple heel? Adv Skin Wound Care 2006;19(1):6.
[25] Gefen A. The biomechanics of heel ulcers. J Tissue Viability 2010;19(4):124–31. https://doi.org/10.1016/j.jtv.2010.06.003.
[26] Greenwood JE. Function of the panniculus carnosus—a hypothesis. Vet Rec 2010;167(19):760. https://doi.org/10.1136/vr.c6210.
[27] Ronald AB, Adel KA, Ryosuke M, Carnosus P. Illustrated encyclopedia of human anatomic variation: opus I: muscular system: alphabetical listing of muscles: P. March 1, 2018. Retrieved From, http://www.anatomyatlases.org/AnatomicVariants/MuscularSystem/Text/P/05Panniculus.shtml.
[28] Spina AA. The plantaris muscle: anatomy, injury, imaging, and treatment. J Can Chiropr Assoc 2007;51(3):158–65.
[29] Moore CW, Rice CL. Structural and functional anatomy of the palmaris brevis: grasping for answers. J Anat 2017;231(6):939–46. https://doi.org/10.1111/joa.12675.
[30] Luboz V, Perrier A, Stavness I, Lloyd JE, Bucki M, Cannard F, et al. Foot ulcer prevention using biomechanical modelling. Comput Methods Biomech Biomed Eng Imag Vis 2014;2(4):189–96. https://doi.org/10.1080/21681163.2013.837410.
[31] Levy A, Frank MB-O, Gefen A. The biomechanical efficacy of dressings in preventing heel ulcers. J Tissue Viability 2015;24(1):1–11. https://doi.org/10.1016/j.jtv.2015.01.001.
[32] Kurihara T, Sasaki R, Isaka T. Mechanical properties of achilles tendon in relation to various sport activities of collegiate athletes. 2012.
[33] Shigekazu I, Keiko I, Mitsuo N. Finite element estimation of pressure distribution inside the trunk on a mattress. 2015. Retrieved April 9, 2018, from https://www.ausmt.org/index.php/AUSMT/article/view/949/462.
[34] Choi PA. Estimation of Young's modulus and Poisson's ratio of soft tissue using indentation. The Hong Kong Polytechnic University; 2009. Retrieved February 20,2018 from http://hdl.handle.net/10397/2777.
[35] Cui L, Maas H, Perreault EJ, Sandercock TG. In situ estimation of tendon material properties: differences between muscles of the feline hindlimb. J Biomech 2009;42(6):679–85. https://doi.org/10.1016/j.jbiomech.2009.01.022.

[36] Rupin F, Saied A, Dalmas D, Peyrin F, Haupert S, Barthel E, Boivin G, Laugier P. Experimental determination of Young modulus and Poisson ratio in cortical bone tissue using high resolution scanning acoustic microscopy and nanoindentation. J Acoust Soc Am 2008;123(No 5) (n.d.). Retrieved February 21, 2018, from https://asa.scitation.org/doi/abs/10.1121/1.2935440.

[37] Beardmore R. Properties of metals. 2010. Retrieved February 21, 2018, from http://www.roymech.co.uk/Useful_Tables/Matter/prop_metals.htm.

[38] Koo TK, Guo J-Y, Cohen JH, Parker KJ. Quantifying the passive stretching response of human tibialis anterior muscle using shear wave elastography. Clin Biomech (Bristol, Avon) 2014;29(1):33−9. https://doi.org/10.1016/j.clinbiomech.2013.11.009.

[39] Hansang K, Lawrence Y, Andrew S, Joseph LD. Determination of poisson ratio of bovine extraocular muscle by computed X-ray tomography. BioMed Res Int 2012;2013. https://doi.org/10.1155/2013/197479. Article ID 197479, 5 pages, 2013.

[40] Nim TH, Luo L, Clément M-V, White JK, Tucker-Kellogg L. Systematic parameter estimation in data-rich environments for cell signalling dynamics. Bioinformatics 2013;29(8):1044−51. https://doi.org/10.1093/bioinformatics/btt083.

[41] Bucki M, Luboz V, Perrier A, Champion E, Diot B, Vuillerme N, Payan Y. Clinical workflow for personalized foot pressure ulcer prevention. Med Eng Phys 2016;38:845−53. https://doi.org/10.1016/j.medengphy.2016.04.017. pdf.